Temporal requirement of *Hoxa2* in cranial neural crest skeletal morphogenesis

Fabio Santagati*, Maryline Minoux*, Shu-Yue Ren‡ and Filippo M. Rijli§

Institut de Génétique et de Biologie Moléculaire et Cellulaire, CNRS/INSERM/ULP, UMR 7104, BP 10142, CU de Strasbourg, 67404 Illkirch Cedex, France

*These authors contributed equally to this work
‡Present address: Center for Biotechnology, College of Science and Technology, Temple University, Philadelphia, PA 19122, USA
§Author for correspondence (e-mail: rijli@igbmc.u-strasbg.fr)

Summary

Little is known about the spatiotemporal requirement of Hox gene patterning activity in vertebrates. In *Hoxa2* mouse mutants, the hyoid skeleton is replaced by a duplicated set of mandibular and middle ear structures. Here, we show that *Hoxa2* is selectively required in cranial neural crest cells (NCCs). Moreover, we used a Cre-ERT2 recombinase system to induce a temporally controlled *Hoxa2* deletion in the mouse. *Hoxa2* inactivation after cranial NCC migration into branchial arches resulted in homeotic transformation of hyoid into mandibular arch skeletal derivatives, reproducing the conventional *Hoxa2* knockout phenotype, and induced rapid changes in *Alx4*, *Bapx1*, *Six2* and *Msx1* expression patterns. Thus, hyoid NCCs retain a remarkable degree of plasticity even after their migration in the arch, and require *Hoxa2* as an integral component of their morphogenetic program. Moreover, subpopulations of postmigratory NCCs required *Hoxa2* at discrete time points to pattern distinct derivatives. This study provides the first temporal inactivation of a vertebrate Hox gene and illustrates Hox requirement during late morphogenetic processes.

Key words: Hox, Cranial neural crest plasticity, Craniofacial development, Mouse, CreERT2, Middle ear, Gonial bone, Skeletal derivatives, Conditional knockout

Introduction

The morphogenesis of the head region involves the neural crest (NC), a unique cell population that represents one of the innovative traits of the vertebrate lineage. Neural crest cells (NCCs) originate from a dorsal level of the developing neural tube and have the distinctive ability to migrate towards various regions of the embryo, where they differentiate into a variety of cellular types and contribute to the ontogenesis of several organs and structures (reviewed by Gammill and Bronner-Fraser, 2003; Le Douarin and Kalcheim, 1999). In particular, a large part of the head and facial skeleton derives from the NCCs of the cranial region. The cranial NCCs migrating from the diencephalon and anterior mesencephalon contribute to the frontonasal mass and skull bones, whereas NCC populations migrating from posterior mesencephalon and hindbrain contribute to the branchial arches and generate facial, jaw and neck bones (reviewed by Santagati and Rijli, 2003).

The way each subpopulation of cranial NCCs acquires the competence to generate distinctive cartilaginous structures and bones represents a fascinating matter of investigation that has inspired seminal experiments and a fervent discussion over the past few decades. By means of chick-to-quail transplants of pre-migratory NCCs, Noden observed that grafting of presumptive first branchial arch NCCs to replace presumptive second arch NCCs resulted in the mirror duplication of first arch skeletal elements in the place of second arch structures (Noden, 1983). This result suggested that NCCs were intrinsically endowed with the potentiality to form specific structures, or pre-patterned, according to their rostrocaudal origin in the neural tube. However, recent work has shown that the surrounding environment provides instructive signals to NCCs in order to trigger their differentiation process, as well as to achieve the correct shaping, positioning and orientation of the developing skeletal structures (Couly et al., 2002; Crump et al., 2004; Ruhin et al., 2003; Trainor et al., 2002). In turn, the NCCs initiate morphogenesis following an intrinsic, species-specific, patterning program that may involve feedback signalling to epithelia (Eames and Schneider, 2005; Ferguson et al., 2000; Schneider and Helms, 2003; Shigetani et al., 2002; Tucker and Lumsden, 2004). Thus, craniofacial morphogenesis appears to be the result of reciprocal signalling between neural crest mesenchyme and the surrounding environment, where timing is an essential component (reviewed by Le Douarin et al., 2004; Santagati and Rijli, 2003). Although a significant advance has been provided by the identification of molecules influencing cranial NCC patterning ability (reviewed by Helms et al., 2005), little is known about the temporal span during which cranial NCCs can generate an appropriate pattern in response to extrinsic stimuli. Another aspect that is poorly understood is how positional information along the anteroposterior axis of distinct subpopulations of NCCs impinges on the patterning programs to give rise to specific subsets of skeletal elements. These issues are related to the

spatiotemporal plasticity of the NCCs during craniofacial development.

An important molecular distinction of cranial NCCs populations along the anteroposterior axis concerns their patterns of Hox gene expression. The NCCs contributing to skull bones, frontonasal and first arch-derived jaw structures do not express Hox genes (Couly et al., 1998) (reviewed by Shigetani et al., 2005). By contrast, NCCs contributing to hyoid and throat skeletal elements derived from the second and more posterior branchial arches, respectively, do express various combinations of Hox genes (Hunt et al., 1991). The involvement of Hox genes in providing rostrocaudal patterning information to branchial arch derivatives first became evident with the targeted inactivation of *Hoxa2* in the mouse (Gendron-Maguire et al., 1993; Rijli et al., 1993). As a result of *Hoxa2* functional depletion, the second arch skeletal elements were homeotically transformed in a duplicated set of first arch-like elements with reverse polarity (Gendron-Maguire et al., 1993; Rijli et al., 1993), strikingly phenocopying the outcome of Noden's heterotopic grafts in the chick. This result indicated that *Hoxa2* acts as a key genetic switch, enabling the patterning of second arch instead of first arch derivatives. *Hoxa2* gain-of-function experiments in the first branchial arch of chick, *Xenopus* and zebrafish embryos yielded a reverse outcome, i.e. second arch-like structures developed in the place of first arch elements, demonstrating a conserved role of *Hoxa2* as a selector of second arch patterning information in vertebrates (Grammatopoulos et al., 2000; Hunter and Prince, 2002; Pasqualetti et al., 2000).

Given the unique role of *Hoxa2*, its mutagenesis in the mouse represents a suitable mammalian genetic model with which to address unsolved questions about the spatiotemporal control of cranial NCC patterning. Here, we set up a conditional mutagenesis system in the mouse, and observed the effects of *Hoxa2* deletion in a tissue- and time-dependent manner. Our analysis yielded several novel insights. First, we found that *Hoxa2* is selectively required in second arch NCCs. Removal of *Hoxa2* in NCCs phenocopied the full knockout transformation of second into first arch morphology. Second, by using a Cre/*loxP*-based system, we temporally induced *Hoxa2* deletion and showed that *Hoxa2* function at pre-migratory stages does not provide NCCs with irreversible information for patterning second arch derivatives. Rather, instruction about shape, size and orientation of second arch skeletal elements is provided after NCC migration. However, the execution of the NCC patterning program is strictly *Hoxa2* dependent. In fact, homeotic changes can still be obtained upon *Hoxa2* inactivation well after NCCs reached their final destination in the second arch. These data illustrate for the first time that second arch NCCs not only retain a degree of plasticity over a remarkably long period, but also that they require the expression of *Hoxa2* as an irreplaceable and integral component of their intrinsic patterning program. Our data also suggest that *Hoxa2* may directly regulate the spatial expression of a number of target genes involved in the morphogenetic process. Finally, we found that *Hoxa2* function is required at separate time points to pattern distinct second arch derivatives. Altogether, this study provides the first temporal analysis of Hox gene function in a vertebrate embryo and illustrates a Hox requirement during late morphogenetic processes.

Materials and methods

Generation of the *CMV-βactin-Cre-ERT2* transgenic line

The *CMV-βactin-Cre-ERT2* (*Cre-ERT2*) transgene was constructed by introducing a 2 kb fragment containing the Cre-ERT2 fusion cassette (Feil et al., 1997) into the *Eco*RI site of the pCX vector, which bears the CMV immediate-early (CMV-IE) enhancer/chicken β-actin basal promoter driving ubiquitous constitutive expression. A *Sal*I-*Sfi*I 4.6 kb fragment containing the whole transgenic construct from the CMV-IE enhancer to the rabbit β-globin poly A signal was purified and used for pronuclear injection into fertilized oocytes of CD1 mice.

Founder animals were identified by PCR amplification with Cre-specific primers and bred onto a C57BL/6 genetic background. Offspring carrying the *Cre-ERT2* transgene were genotyped by PCR. Nine distinct founder transgenic lines were characterized for integration of the transgene by Southern blot hybridization and for ubiquitous expression of the *Cre-ERT2* mRNA by in situ hybridization. The functionality of the Cre-ERT2 fusion protein upon tamoxifen induction was ascertained by crossing it with a ROSA 26R (Soriano, 1999) reporter line. Embryos collected as early as 24 hours after treatment carrying both the ROSA 26R reporter allele and the *Cre-ERT2* transgene stained ubiquitously upon X-gal exposure (data not shown). Conversely, no staining was observed on control untreated embryos from the same intercross (not shown). Three transgenic lines (F34, F85 and F105a) were selected after this screening. The data presented in this work were primarily obtained using the F34 line, although the F85 line was used for confirmation purposes when needed. No noticeable differences in the outcomes were observed using the two lines.

Mating scheme

The *Cre-ERT2* and the *Wnt1-Cre* (Danielian et al., 1998) transgenic lines were crossed with either the *Hoxa2^EGFPfloxNeo* knock-in (Pasqualetti et al., 2002) or the *Hoxa2^flox* conditional alleles (Ren et al., 2002) for the different experimental purposes. To obtain *Hoxa2* conditional homozygous mutant mice, a first breeding round was accomplished to generate compound *Hoxa2^flox/+;Cre-ERT2* or *Hoxa2^flox/+;Wnt1-Cre* mice, respectively. These animals were in turn mated to *Hoxa2^flox/flox* mice. Homozygous mutant newborns were obtained with an expected Mendelian ratio. All genotypes were determined by PCR.

Tamoxifen treatment

Tamoxifen (Sigma) was dissolved in pre-warmed corn oil (Sigma) to make a 20 mg/ml solution and stored at 4°C. Tamoxifen was administered orally to pregnant females by means of a gavage syringe. Optimal doses for the different developmental stages were experimentally determined as described in the Results section. In particular, the amount of administered tamoxifen per pregnant female (about 35-40 g of body weight) was estimated as follows: 5 mg at 7.0 dpc, 6 mg at 8.0 dpc, 7 mg at 9.5 dpc, 8 mg at 10.0 dpc, 9 mg at 10.5 dpc and 10 mg at 11.0 dpc. To obtain maximal Cre-ERT2 recombination efficiency at later embryonic stages, double (10 mg at 11.5 dpc and 12.0 dpc) and triple (10 mg at 12.5 dpc, 13.0 dpc and 13.5 dpc) successive administrations (chronic treatment) were provided with 12-hour intervals. For precise embryonic stage estimation at the time of treatment, mated females were checked for vaginal plugs every 2 hours. The time of a detected plug was considered as embryonic day 0. Specimens were collected at the desired time after the last treatment.

Skeletal preparation

Neonatal mice were skinned and eviscerated. Skeletons were fixed overnight in 95% ethanol and then stained in Alcian Blue (750 μg/ml in 80 ml of 95% ethanol, 20 ml of glacial acetic acid) for at least 24 hours. Skeletons were cleared in 2% KOH for 8-10 hours, then 1% KOH overnight and then stained in Alizarin Red (100 μg/ml in 1% KOH) overnight. Further clearance was performed in 20%

glycerol/1% KOH. Skeletons were stocked in 50% glycerol/50% ethanol.

Immunohistochemistry

Immunostaining for EGFP on cryosections was performed using a polyclonal rabbit anti-GFP antibody (Molecular Probes Europe BV) and a peroxidase-conjugated goat anti-rabbit IgG secondary antibody (Beckman Coulter France SA). Detection was performed with DAB chromogen (DAKO SA).

In situ hybridisation

In situ hybridisation on whole-mount embryos and cryosections was performed as previously described (Samad et al., 2004). The following RNA probes were used: *Hoxa2* (Ren et al., 2002), *Alx4* (Qu et al., 1997), *Bapx1* (*Nkx3.2*) (Lettice et al., 2001), *Msx1* (Robert et al., 1989), *Six2* (Oliver et al., 1995).

Results

Selective deletion of *Hoxa2* in second arch neural crest cells is sufficient to induce second-to-first arch homeosis

Most of the defects of the *Hoxa2* knockout mice concern structures of NC origin, including the skeletal elements of the second branchial arch and the external ear pinna (Rijli et al., 1993; Gendron-Maguire et al., 1993). Nevertheless, in addition to in NCCs, *Hoxa2* is also expressed in the neural epithelium, where NCCs arise, and in the branchial arch surface ectoderm (Couly et al., 1998; Hunt et al., 1991; Pasqualetti et al., 2000; Prince and Lumsden, 1994). Such tissues are likely to exhibit a cross-talk interaction with the NCCs and to influence their morphogenetic potential. To ascertain whether the *Hoxa2* mutant phenotype is entirely generated by the lack of *Hoxa2* function in the NCCs, or if it is partially contributed by *Hoxa2* loss in neighboring tissues, we conditionally ablated *Hoxa2* in the NCC population. For this purpose, we mated mice homozygous for a previously described *Hoxa2flox* allele (Ren et al., 2002) to a *Wnt1-Cre* transgenic line, expressing the Cre recombinase in NCC precursors at the dorsal folds of the neuroepithelium (Danielian et al., 1998). In *Hoxa2flox/flox;Wnt1-Cre* 10.5 day post coitum (dpc) embryos, *Hoxa2* expression was selectively abolished from the NCCs contributing to the second and more posterior arches, as assessed by whole-mount in situ hybridisation (Fig. 1C) (see also Ren et al., 2002). At birth, *Hoxa2flox/flox;Wnt1-Cre* mutant mice displayed a similar external phenotype to the conventional *Hoxa2−/−* mutants (Rijli et al., 1993), namely the loss of external ear (Fig. 4C). Also, the analysis of skeletal preparations from *Hoxa2flox/flox;Wnt1-Cre* mutant pups revealed the same set of malformations as in *Hoxa2−/−* mice. Namely, the second arch-derived stapes, styloid process, and lesser horns of the hyoid bone were absent and replaced by a duplicated set of first arch-like structures with reverse polarity, including a duplicated incus, malleus, tympanic bone, a transformed gonial bone, and a partially duplicated Meckel's cartilage (Fig. 1F,I).

Thus, *Hoxa2* is selectively required in second arch NCCs. *Hoxa2* inactivation in NCCs is sufficient to yield the defects associated with middle and external ear development, while expression of *Hoxa2* in adjacent tissues does not alleviate the overall mutant phenotype.

Temporally controlled deletion of the *Hoxa2* locus

In order to carry out a time-course mutagenesis of the *Hoxa2* gene, we generated the transgenic mouse line *CMV-βactin-Cre-ERT2 (Cre-ERT2)* bearing a tamoxifen (TM)-inducible form of *Cre* recombinase, *Cre-ERT2* (Feil et al., 1997), driven by the ubiquitous chicken β-actin promoter. Transgenic lines expressing *Cre-ERT2* can be efficiently used to perform time-specific excision of a target gene by a Cre/*loxP*-based conditional knockout system (reviewed by Metzger et al., 2005). We tested the efficiency of the Cre-ERT2 recombinase in mediating excision at the *Hoxa2* locus by directly monitoring the levels of residual *Hoxa2* mRNA in TM-induced *Hoxa2flox/flox;Cre-ERT2* embryos. The doses and conditions of TM treatment (see Materials and methods) were optimized for different developmental time points on the basis of the maximal degree of Cre-ERT2-induced loss of expression of *Hoxa2*, as detected by whole-mount or tissue section in situ hybridisation. Tamoxifen was administered to pregnant females at 9.5, 10.5 and 11.0 dpc (single gavage), as well as at
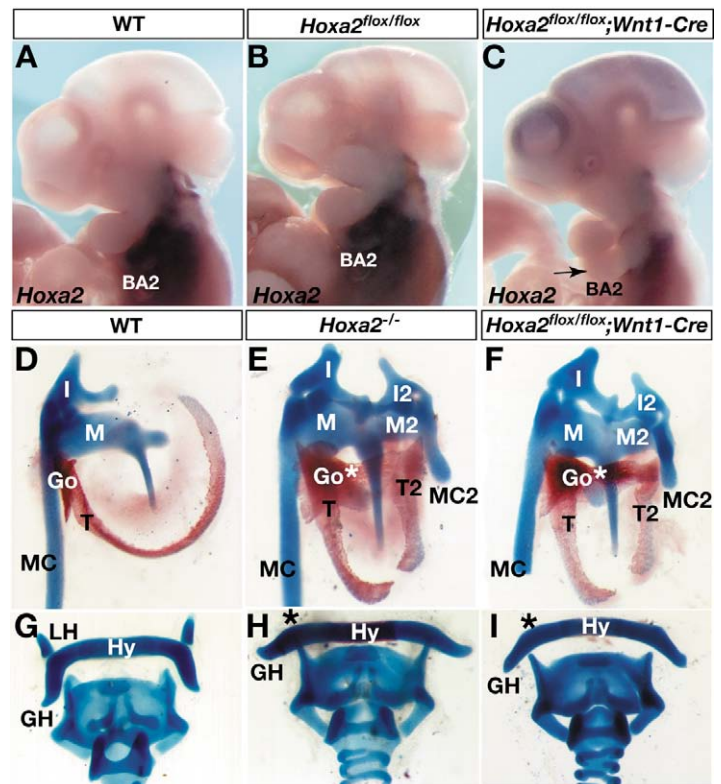

Fig. 1. Neural crest-specific *Hoxa2* knockout. (A-C) In situ hybridization on wild-type (A), *Hoxa2flox/flox* (B) and *Hoxa2flox/flox;Wnt1-Cre* (C) whole-mount 10.5 dpc embryos using an antisense *Hoxa2* probe. In C, *Hoxa2* expression is selectively lost in the NC-derived mesenchyme of the second (arrow) and posterior branchial arches. (D-I) Middle ear (D-F) and hyoid (G-I) skeletal preparations from wild-type (D,G), *Hoxa2−/−* (E,H) and *Hoxa2flox/flox;Wnt1-Cre* (F,I) 18.5 dpc fetuses. Normal structures are indicated: MC, Meckel's cartilage; M, malleus; I, incus; T, tympanic bone; Go, gonial bone; Hy, hyoid bone, with lesser (LH) and greater (GH) horns. In F,I, *Hoxa2flox/flox;Wnt1-Cre* mutants show an identical phenotype to the conventional *Hoxa2−/−* mutants (Rijli et al., 1993), i.e. homeotic duplication of malleus (M2), incus (I2), tympanic bone (T2), partial duplication of Meckel's cartilage (MC2), transformation of gonial bone (Go*), and loss of lesser horns of the hyoid bone (asterisk in H and I).

Development

11.5 or 12.5 dpc (chronic administration; see Materials and methods), and embryos were collected 24 hours after the last
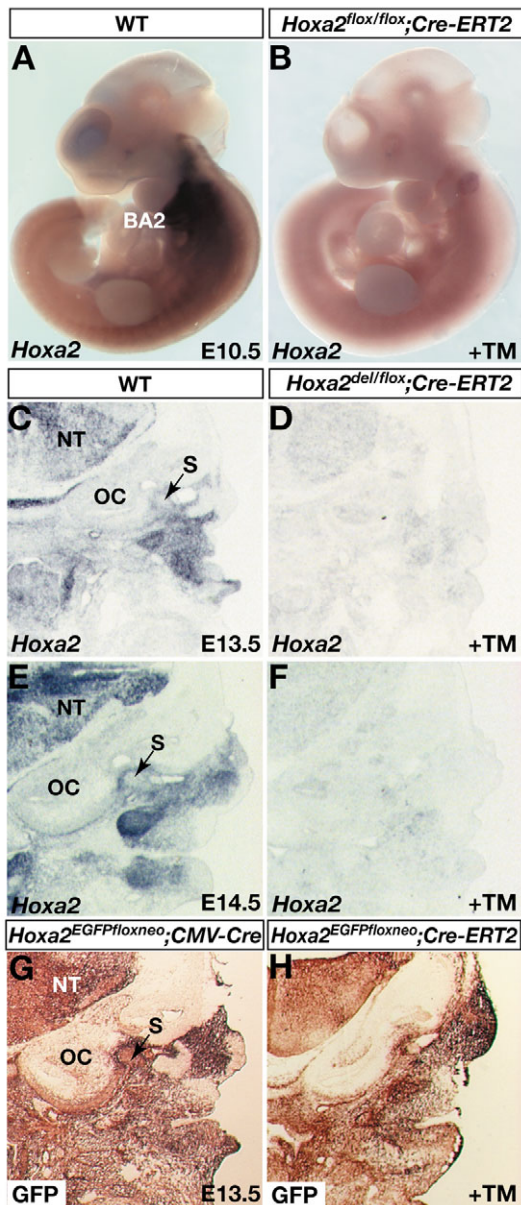

Fig. 2. Tamoxifen-induced deletion of the *Hoxa2* locus. (A-F) In-situ hybridization on whole mounts (A,B) and frontal cryosections (C-F) of mouse embryos using an antisense *Hoxa2* probe. Wild-type embryos at 10.5 (A), 13.5 (C) and 14.5 (E) dpc show strong *Hoxa2* expression in the second (BA2) and posterior branchial arches (A), as well as in the neural tube (NT) and middle ear regions (C,E), respectively. Significant loss of *Hoxa2* transcripts is observed in 10.5 dpc *Hoxa2$^{flox/flox}$;Cre-ERT2* embryos (i.e. carrying two alleles to be excised) after tamoxifen (TM) treatment at 9.5 dpc (B), as well as in 13.5 (D) and 14.5 (F) dpc *Hoxa2$^{del/flox}$;Cre-ERT2* embryos (i.e. carrying only one allele to be excised) after TM treatment at 11.5 and 12.5 dpc, respectively. (G,H) Immunostaining on frontal cryosections of *Hoxa2^{EGFPfloxNeo};CMV-Cre* (G) and *Hoxa2^{EGFPfloxNeo};Cre-ERT2* (H) 13.5 dpc mouse embryos using an anti-GFP antibody. Note that the distribution of TM-induced GFP expression in H is comparatively similar to the constitutive GFP expression in G. OC, otic capsule; S, stapes.

TM administration. We detected no or very little residual *Hoxa2* expression as a result of Cre-ERT2 induction at any of the selected time points (Fig. 2B,D,F; and data not shown).

In addition, the effectiveness of the *Hoxa2* excision was confirmed by means of a complementary Cre-ERT2-induced 'gain-of-expression' approach. To this aim, we cross-mated our *Cre-ERT2* transgenic line with the *Hoxa2^{EGFPfloxNeo}* line, in which the expression of the EGFP reporter, knocked-in at the *Hoxa2* locus, is induced only upon Cre-mediated excision of the adjacent floxed *Neo* cassette (Pasqualetti et al., 2002). *Hoxa2^{EGFPfloxNeo};Cre-ERT2* embryos were collected 24 hours after the last TM administration. The spatial extent of EGFP activation was compared with that of control specimens of similar stages obtained by mating the *Hoxa2^{EGFPfloxNeo}* knock-in line with a *CMV-Cre* transgenic line (Dupe et al., 1997). Both constitutive and induced Cre activities gave rise to similar EGFP immunostaining patterns throughout the *Hoxa2* expression domain. In particular, EGFP staining in the second arch from both genotypes was indistinguishable at any of the probed stages (Fig. 2G,H; and data not shown).

Distinct temporal requirements of *Hoxa2* in the patterning of second arch structures

In the mouse, *Hoxa2* is expressed in second arch NCCs from the onset of their migration (Maconochie et al., 1999) through the stage of prechondrogenic condensation (Kanzler et al., 1998). When chondrogenesis begins, *Hoxa2* is downregulated in the cells that undergo differentiation, whereas it remains expressed in the NC-derived surrounding mesenchyme (Kanzler et al., 1998) until at least 14.5 dpc (Fig. 2E), a stage at which chondrogenesis is well underway.

To address the temporal requirement of *Hoxa2* in NC patterning, pregnant females were given tamoxifen at different doses and gestational stages following the scheme described above (see also Materials and methods), and *Hoxa2$^{flox/flox}$;Cre-ERT2* fetuses or newborns were collected and analysed for mutant phenotypes.

We started by inducing *Hoxa2* deletion after TM treatment at 7.0 dpc. TM induces Cre-ERT2 translocation to the nucleus within 6 hours, it reaches its maximal accumulation at about 24 hours and is still present after about 36 hours (Hayashi and McMahon, 2002; Zervas et al., 2004). Considering that skeletogenic NC migration in the mouse begins at around 8.25 dpc (Serbedzija et al., 1992), TM treatment at 7.0 dpc was expected to induce efficient *Hoxa2* inactivation before the onset of NCC migration, and therefore to reproduce the phenotypes of conventional and conditional *Wnt1-Cre*-induced *Hoxa2* knockouts. As anticipated, the TM-induced *Hoxa2$^{flox/flox}$;Cre-ERT2* mutant newborns died perinatally, and displayed mirror image duplication of first arch-like structures and absence of external ear pinna (Fig. 3C; and data not shown). This outcome confirmed that the TM-inducible targeting system could be efficiently employed to induce a full *Hoxa2* knockout phenotype. Conversely, no morphological abnormalities were detected in *Hoxa2$^{flox/flox}$;Cre-ERT2* newborn mice that did not undergo TM treatment (Fig. 3B).

Next, we tested the effect of *Hoxa2* inactivation at NC post-migratory stages. We started with TM treatment at 9.5 dpc. By this stage, skeletogenic NCCs have already completed their migration (Serbedzija et al., 1992) and filled the branchial arches. Notably, deletion of *Hoxa2* at this stage also yielded a
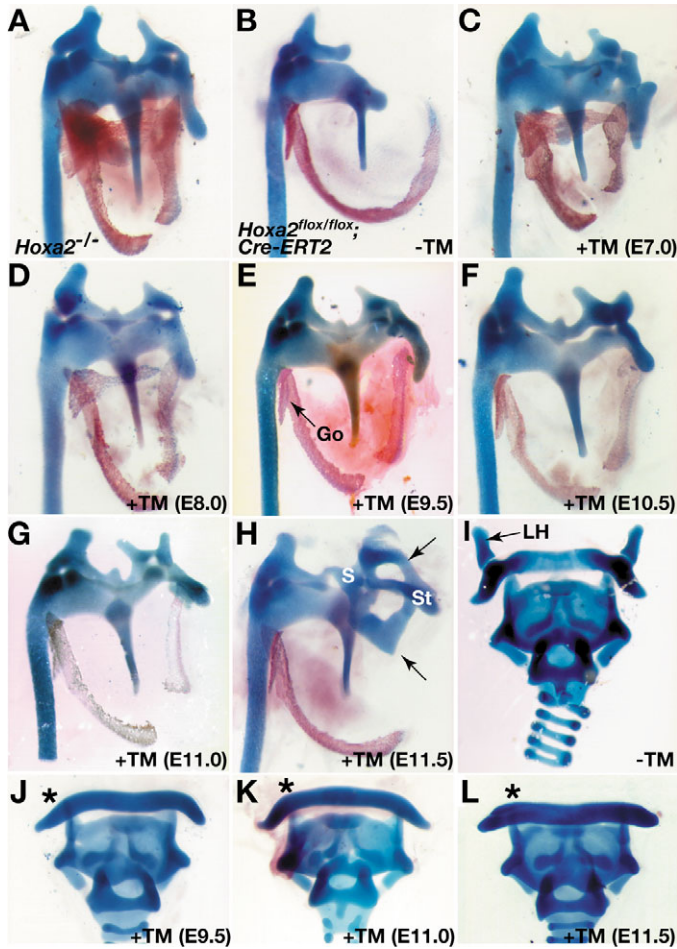
Fig. 3. Middle ear and hyoid skeletal changes in tamoxifen-induced *Hoxa2* mutant mice. Middle ear (A-H) and hyoid (I-L) skeletal preparations from 18.5 dpc fetuses are shown.
(B-G) *Hoxa2^{flox/flox}*;*Cre-ERT2* homozygous mutant fetuses in the absence (B) and presence (C-G) of TM treatment at different time points from 7.0 dpc up to 11.0 dpc, as indicated. Although untreated *Hoxa2^{flox/flox}*;*Cre-ERT2* mice have normal middle ear bones (B; compare with Fig. 1D), homeotic duplications comparable to those of the conventional *Hoxa2^{-/-}* mutant (A) are observed in C,D. In E-G, the gonial bone (Go, arrow in E) is no longer transformed in fetuses treated from 9.5 dpc onwards, while the remaining cartilage and dermal bone elements are duplicated. By contrast, *Hoxa2^{flox/flox}*;*Cre-ERT2* fetuses treated at 11.5 dpc (H) do not show any duplication. In H, malformed second arch structures, including stapes (S) and styloid process (St), are often fused to additional ectopic cartilages (arrows), while duplication of dermal bones is not observed. Asterisks in J-L show the loss of the lesser horns (LH) of the hyoid bone in *Hoxa2^{flox/flox}*;*Cre-ERT2* 18.5 dpc fetuses treated at 9.5 dpc (J), 11.0 dpc (K) and 11.5 dpc (L), similar to in conventional *Hoxa2^{-/-}* mutants (Fig. 1H). These structures are present in untreated *Hoxa2^{flox/flox}*;*Cre-ERT2* mice (arrow in I).

lack of external ear pinna and homeotic replacement of second with first arch-like structures (Fig. 3E,J). Interestingly, the only distinct feature in the middle ear skeleton of 'post-migratory' *Hoxa2^{flox/flox}*;*Cre-ERT2* mutants was a rather normal looking gonial bone (Fig. 3E). In the conventional and 'pre-migratory' *Hoxa2* mutants, this membranous bone appears, on the contrary, transformed, as it is abnormally enlarged and

stretches across, bridging over the two halves of the mirror duplication (Rijli et al., 1993) (Fig. 1E,F, Fig. 3A). Notably, deletion of *Hoxa2* by TM treatment at 8.0 dpc resulted in a variable gonial bone phenotype, ranging from a malformed gonial bone to a complete transformation of the element (Fig. 3D; data not shown). These results indirectly identify a time window for gonial bone specification and indicate that the first arch NCCs contributing to this membranous element may be irreversibly committed at an early migratory stage, before the NCCs give rise to the other elements of the middle ear region.

We further investigated the effect of *Hoxa2* inactivation at later developmental stages. Remarkably, conditional *Hoxa2* deletion induced by TM treatment after NCC migration at 10.5 and even at 11.0 dpc still resulted in the duplication of middle ear elements, with the exception of the gonial bone, and in a lack of the lesser horns of the hyoid bone (Fig. 3F,G,K), similar to the outcome of the TM treatment at 9.5 dpc. By contrast, in embryos treated at 11.5 dpc, duplicates of the tympanic and squamosal bones were no longer observed, whereas the second arch cartilaginous derivatives were still affected (Fig. 3H; and data not shown). Specifically, the lesser horns of the hyoid bone were missing (Fig. 3L) while, interestingly, the stapes and the styloid process were malformed and associated with ectopic cartilage (arrows in Fig. 3H), perhaps representing an intermediary state towards the generation of duplicated first arch-like middle ear elements. Finally, in newborns treated at 12.5 dpc, the second arch skeletal elements were only mildly affected (data not shown). The analysis at 11.5 and 12.5 dpc was also carried out on mice bearing a fully deleted and a floxed allele (*Hoxa2^{del/flox}*;*Cre-ERT2*), so that only one allele, instead of two, was to be excised. The results were comparable to those obtained with *Hoxa2^{flox/flox}*;*Cre-ERT2* fetuses (data not shown). Moreover, analysis by in situ hybridisation in late-treated embryos confirmed an essentially complete loss of *Hoxa2* expression (Fig. 2D,F). Thus, the obtained phenotypes did not appear to be due to partial Cre-mediated recombination; rather, they unveiled distinct temporal requirements for *Hoxa2* in patterning individual skeletal elements and subsets of NCCs populations of the second arch.

The external ear was systematically affected in all TM-induced *Hoxa2* mutants. In particular, *Hoxa2* mutagenesis induced by TM treatment up to 11.5 dpc always resulted in the loss of the pinna (Fig. 4D,E). In addition, mutant pups obtained by chronic tamoxifen treatments between 12.5 and 13.5 dpc displayed a smaller external ear (Fig. 4F). This indicated a late role of *Hoxa2* in the morphogenesis of the external ear pinna, temporally distinct from its involvement in middle ear patterning.

Altogether, these results have revealed an unprecedented plasticity of second arch NCCs, even after they completed their migration. They have also shown that the execution of their morphogenetic program is absolutely dependent on *Hoxa2* function at post-migratory stages. Moreover, our data indicate that *Hoxa2* exerts temporally distinct functions on specific subpopulations of NCCs within the second arch, each giving rise to individual skeletal elements or external ear structures.

Hoxa2 inactivation at post-migratory stages results in rapid molecular changes in downstream target genes

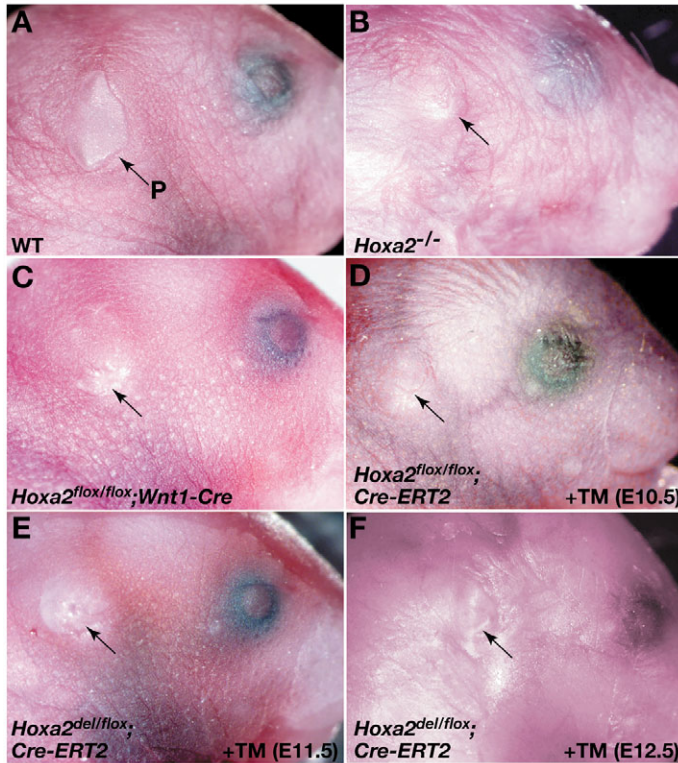The finding that *Hoxa2* acts at late developmental stages, in

Fig. 4. Morphological changes of external ear pinna in conditional *Hoxa2* mutant mice. (A-F) Analysis of the external ear phenotype in newborn mice. Lateral view of the head of wild-type (A), *Hoxa2*⁻/⁻ (B) and *Hoxa2*^flox/flox^;*Wnt1-Cre* (C), as well as *Hoxa2*^flox/flox^;*Cre-ERT2* (D) and *Hoxa2*^del/flox^;*Cre-ERT2* (E,F) newborn mice treated with tamoxifen (TM) at various stages, as indicated between brackets. The arrows show absent (B-E) or hypoplastic (F) ear pinna in mutant mice, according to the stage of induction. P, pinna.

concomitance with the onset of the morphogenetic process, prompted us to investigate whether *Hoxa2* may be an integral component of the NCC molecular patterning program. In particular, we asked whether *Hoxa2* could be directly involved in the generation of the second arch-specific molecular pattern in post-migratory NCCs by regulating the spatial expression of genes involved in branchial arch patterning.

We searched for genes displaying asymmetrical expression patterns in the first and second arch NCC mesenchyme at around the time when morphogenesis is beginning. We first tested whether their expression patterns could be selectively altered in the conventional *Hoxa2*⁻/⁻ mutant. Interestingly, genes exclusively or predominantly expressed in the first arch, such as the homeobox genes *Alx4*, *Bapx1* and *Six2*, were found to be ectopically expressed in the second arch of *Hoxa2*⁻/⁻ 10.5 dpc embryos (Fig. 5B,E,K). Conversely, *Msx1*, which has a broader expression pattern in the hyoid than in the mandibular arch, was downregulated to a first arch-like pattern in the second arch of *Hoxa2*⁻/⁻ embryos (Fig. 5H).

Next, we asked whether the expression pattern changes were the consequence of post-migratory *Hoxa2* lack of function. We, therefore, induced the *Hoxa2* mutation in 9.5 dpc embryos, collected them 24 hours later, and performed whole-mount in situ hybridisation for the selected genes. Postmigratory *Hoxa2* inactivation was sufficient to induce similar expression pattern
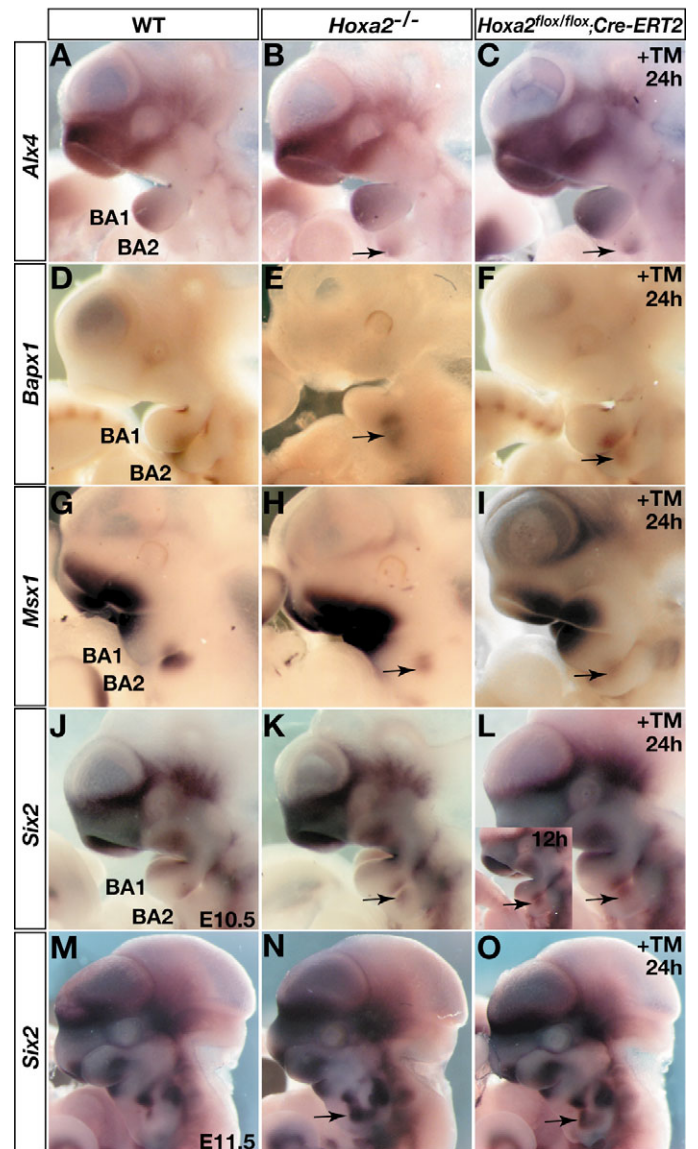

Fig. 5. Molecular changes in the second branchial arch of conventional and tamoxifen-induced *Hoxa2* mutant embryos. (A-L) Whole-mount in situ hybridization on wild-type (A,D,G,J), *Hoxa2*⁻/⁻ (B,E,H,K) and TM-treated *Hoxa2*^flox/flox^;*Cre-ERT2* (C,F,I,L) 10.5 dpc embryos using *Alx4* (A-C), *Bapx1* (D-F), *Msx1* (G-I) and *Six2* (J-L) antisense probes. *Hoxa2*^flox/flox^;*Cre-ERT2* homozygous mutant embryos were collected 24 hours or 12 hours (inset in L) after TM treatment. Arrows show *Alx4*, *Bapx1* and *Six2* ectopic expression, as well as *Msx1* downregulation in the second arch of both *Hoxa2*⁻/⁻ and TM-treated *Hoxa2*^flox/flox^;*Cre-ERT2* mutant embryos. (M-O) Whole-mount in situ hybridization on wild-type (M), *Hoxa2*⁻/⁻ (N) and TM-treated *Hoxa2*^flox/flox^;*Cre-ERT2* (O) 11.5 dpc embryos with a *Six2* probe. The *Hoxa2*^flox/flox^;*Cre-ERT2* mutant embryo in O was treated at 10.5 dpc. Arrows show ectopic expression in the second arch of both *Hoxa2*⁻/⁻ and *Hoxa2*^flox/flox^;*Cre-ERT2* embryos. BA1, first branchial arch; BA2, second branchial arch.

changes of *Alx4*, *Bapx1*, *Six2* and *Msx1* to those detected in conventional *Hoxa2* knockout embryos (Fig. 5C,F,I,L), providing molecular support to the morphological transformation of skeletal structures observed in newborns

following a similar TM treatment (Fig. 3). Most interestingly, we obtained similar molecular results by treating embryos at 10.0 dpc and collecting them as early as 12 hours after TM administration (shown for *Six2* in Fig. 5L, inset; and data not shown). Such a rapid molecular reorganisation of second arch mesenchyme as a result of *Hoxa2* inactivation in post-migratory NCCs suggests that these genes may be direct targets of *Hoxa2*.

Finally, we performed whole-mount in situ hybridisation on 11.5 dpc embryos after TM-induced *Hoxa2* deletion at 10.5 dpc. Yet again, the second arch gene expression pattern switched to a first arch-like pattern (shown for *Six2* in Fig. 5O; and data not shown). Thus, although a second arch-specific *Hoxa2*-dependent molecular pattern has been already set up by 10.5 dpc, this last result further underscores that NCCs are not yet irreversibly fated towards a definite morphogenetic program, rather they are still susceptible to molecular changes that can revert their developmental program.

Discussion
Hoxa2 expression is necessary in neural crest cells for the selection of a hyoid instead of mandibular program

We have shown that *Hoxa2* depletion in NCCs is sufficient to induce a full knockout phenotype, as in the conventional *Hoxa2⁻/⁻* mice. *Hoxa2*-deficient NCCs give rise to first arch-like structures, in place of second arch elements, regardless of whether they originate from or migrate into a Hox-expressing environment. This finding demonstrates not only that the main role of the gene is fulfilled within the NCCs themselves, but it also gives evidence for *Hoxa2* being part of a NCC inherent genetic program, which will eventually determine the morphogenetic fate of the cells. This finding allows a better understanding of the outcome of previous experiments. For instance, recent work has shown the role of signals arising from neighbouring epithelia in providing instructive patterning information for NCC derivatives (Couly et al., 2002; Hu et al., 2003; Trainor and Krumlauf, 2000; Trainor et al., 2002; Trumpp et al., 1999; Tucker et al., 1999; Pasqualetti and Rijli, 2002; Shigetani et al., 2002). In particular, the pharyngeal endoderm is a source of patterning signals that are distributed along the rostrocaudal axis and influence both Hox-positive and Hox-negative NCC mesenchyme (Couly et al., 2002; Ruhin et al., 2003). Our data show that the loss of expression of *Hoxa2* in NCCs of the second arch is alone responsible for the selection of a first versus second arch morphogenetic program. This indirectly indicates that at least part of the second and first arch NCCs respond to the same set of epithelial signals, and that their distinct readouts solely depend on whether *Hoxa2* is switched on or off (see also below). This finding helps to explain why a Hox-negative NCC population still forms first arch-like structures in a second arch environment (Couly et al., 1998; Noden, 1983).

Tissue specific mutagenesis will still be required to investigate what is the contribution of *Hoxa2* expression in other tissues, if any, to NCC patterning. Also, given that *Hoxa2* is necessary in mouse NCCs to impart a second arch program, it would be interesting to ascertain whether it might also be sufficient. In this respect, it should be noted that ectopic *Hoxa2* overexpression in *Xenopus*, chick and zebrafish embryos resulted in first-to-second arch transformation, although only when all first arch tissues were targeted (Couly et al., 1998; Creuzet et al., 2002; Grammatopoulos et al., 2000; Hunter and Prince, 2002; Pasqualetti et al., 2000). Targeted *Hoxa2* overexpression selectively in first arch NCCs will be required in order to assess such a model in the mouse.

Temporal analysis of Hoxa2 function reveals plasticity of second arch neural crest cells even after their migration

We applied an inducible Cre-ERT2-based approach to achieve time-dependent inactivation of a conditional allele of *Hoxa2*. By this means, we were able to carry out for the first time a functional analysis of the temporal requirement of a Hox factor in a vertebrate embryo. Hox genes are known to play a fundamental role in providing segmental identity at early developmental stages in the vertebrate embryo (Krumlauf, 1994), but little information is available about their potential involvement in late aspects of morphogenetic processes. The importance of this type of study has been recently addressed in a work reporting the conditional inactivation of *Hoxb1* in neurogenic NCCs (Arenkiel et al., 2004). The authors performed their conditional mutagenesis by employing pre- and post-migratory NCC Cre transgenic lines under the control of two distinct promoters from the *Wnt1* and *Ap2* genes, respectively. However, in this type of approach a precise stage-specific dissection of the role of the gene was precluded. On the one hand, the Cre-ERT2-based recombination approach is an efficient and reliable system for temporally controlled, inducible Cre activity both in adult mouse tissues and developing embryos (Ahn and Joyner, 2004; Danielian et al., 1998; Feil et al., 1997; Hayashi and McMahon, 2002; Imai et al., 2001; Kimmel et al., 2000; Metzger et al., 2005; Sgaier et al., 2005). On the other hand, the use of Cre-ERT2 recombinase regulated by a ubiquitous promoter does not consent, on its own, for a tissue-restricted analysis. In this respect, the finding that the conditional inactivation of *Hoxa2* with a *Wnt1*-Cre line resulted in a full knockout phenotype strongly indicates that the abnormalities observed in our time-dependent mutagenesis are mainly due to the disruption of *Hoxa2* activity in the NCC population.

In the mouse, *Hoxa2* expression in second arch NCCs is present from the time of their emergence from the neural folds, at around 8.25 dpc (Maconochie et al., 1999; Nonchev et al., 1996). We show that such an early expression does not provide NCCs with irreversible patterning information. In fact, induction of the *Hoxa2* deletion at post-migratory stages up to at least 11.0 dpc is still sufficient to generate morphological changes substantially similar to those obtained in embryos in which *Hoxa2* is knocked out from NCC pre-migratory stages. Thus, mouse *Hoxa2* is mainly required after the process of NCC migration, in keeping with the maintenance of its expression through at least 14.5 dpc (Fig. 2) (see also Kanzler et al., 1998), a stage at which cartilage differentiation and morphogenesis are underway. This finding also supports the conclusions from the complementary gain-of-function experiments performed on *Xenopus* embryos, in which it was shown that ectopic overexpression of *Hoxa2* mRNA in the Hox-negative first branchial arch could still cause a homeotic first-to-second arch transformation, even at stages subsequent to NCC migration (Pasqualetti et al., 2000).

Most interestingly, the current work reveals for the first time that second arch NCCs maintain plasticity over a remarkably long period, until they undergo skeletal differentiation in the branchial arch, and that they do so irrespective of any previous expression of *Hoxa2*. As we demonstrate that *Hoxa2* is required after NCC migration, our results strongly suggest that *Hoxa2* expression in NCCs is necessary for the molecular interpretation of the information provided by the surrounding environment to yield a second arch-specific morphogenetic program. This model integrates the concept of NCC plasticity with the existence of a NC-specific inherent genetic program that responds to extrinsic stimuli taking into account the developmental history and positional origin of distinct NCC subpopulations.

Distinct temporal and qualitative requirements of *Hoxa2* for the morphogenesis of second arch structures

Vertebrate Hox genes are known to confer anteroposterior positional values to developing tissues, but little is known about how their function is implemented (Knosp et al., 2004; Samad et al., 2004; Stadler et al., 2001; Wellik et al., 2002). We show that this function can be accomplished by a localized morphogenetic activity, which, in the case of *Hoxa2*, is integral to the control of the shape, size and location of the skeletal elements of the second branchial arch.

An important aspect of our study is that we unveiled a differential temporal effect of *Hoxa2* inactivation on cartilage and membranous bone development. Indeed, conventional knockout and gain-of-function studies suggested that *Hoxa2* is involved in patterning cartilaginous elements (Grammatopoulos et al., 2000; Hunter and Prince, 2002; Pasqualetti et al., 2000; Rijli et al., 1993), while at the same time mediating a general inhibitory activity on membranous bone formation (Creuzet et al., 2002; Kanzler et al., 1998). We now show that these two roles can be temporally dissected. In particular, intramembranous bone formation can be ectopically induced in the second arch by *Hoxa2* inactivation up to 11.0 dpc, although not beyond this stage, whereas it is still possible to affect cartilage patterning by TM treatment until at least 11.5 dpc (Fig. 3). This observation indicates that intramembranous bone NC-derived precursors may be specified earlier then cartilage precursors. This is in keeping with the timing of appearance of the early osteoblast differentiation marker *Cbfa1* (*Runx2*), whose expression in the maxillary and mandibular components of the first branchial arch can be detected as early as 11.5 dpc (Otto et al., 1997). In the *Hoxa2*$^{-/-}$ mutant, *Cbfa1* is ectopically expressed in the second branchial arch, implying an inhibitory role of *Hoxa2* on the activation of the osteogenic marker (Kanzler et al., 1998). Thus, the fact that ectopic membranous osteogenesis can be triggered in the second arch by TM-treatment not later than 11.0 dpc (Fig. 3G) strongly suggests that commitment of NCCs to an osteogenic fate occurs close to or at the time when *Cbfa1* expression is induced, that is around 11.5 dpc, even though the first osteogenic differentiation markers will not appear before 13.0 dpc (Bialek et al., 2004). Beyond 11.5 dpc, second arch NCC precursors devoid of *Hoxa2* expression are apparently not able to engage into an osteogenic program (Fig. 3H), either because the inducing signal is not available or possibly because the NCCs have lost their responsiveness.

The inhibition of gonial bone formation represents the sole indication of an early function for *Hoxa2*, as TM-treatment from 9.5 dpc on did not result in gonial bone transformation (Fig. 3E). It is not clear how the NCCs that will originate the gonial condensation are specified during their migratory phase or entry in the arch. In fact *Bapx1*, a gene whose expression in the mouse is associated with incudo-mallear articulation and gonial bone development (Tucker et al., 2004), is not detected in the arches until 10.5 dpc, and it is still ectopically activated in the second arch subsequent to post-migratory *Hoxa2* inactivation (Fig. 5; see below). It is therefore conceivable that *Bapx1* is necessary but not sufficient to promote gonial bone development, and that it requires some other early factor, whose expression can be irreversibly inhibited by *Hoxa2* in the presumptive second arch NCCs during or soon after their migration.

Finally, we have shown that *Hoxa2* inactivation up to 11.5 dpc can still result in a loss of the pinna, similar to in conventional *Hoxa2*$^{-/-}$ mice, although homeosis of middle ear elements is no longer observed. Moreover, external ear development can still be affected by *Hoxa2* inactivation, even at later stages, resulting in a hypomorphic pinna, whereas middle ear ossicles are normally generated (Fig. 4; and data not shown). Thus, *Hoxa2* might be involved in the morphogenesis of the second arch ectomesenchyme, contributing to the pinna through advanced developmental stages, later than its requirement for middle ear patterning. Future studies will be required to assess the molecular pathways regulated by *Hoxa2* in external ear morphogenesis.

Hoxa2 is a positive and negative regulator of gene expression in second arch mesenchyme

The gene expression analysis conducted in this work has provided additional insights on the molecular program regulated by *Hoxa2* in the second arch. Previous studies reported that first arch specific genes can be ectopically activated in the second arch territory of *Hoxa2* mutant embryos (Bobola et al., 2003; Kutejova et al., 2005). Thus, it has been proposed that *Hoxa2* has a mainly repressive role in the second arch NCCs, and that in some cases it is directly implicated in transcriptional inhibition, as with respect to *Six2* (Kutejova et al., 2005). We found here that additional first arch-specific homeobox containing genes, such as *Alx4* and *Bapx1*, are similarly repressed by *Hoxa2*. However, the expression of *Msx1*, which is normally higher and displays a broader distribution in the hyoid than in the mandibular arch at 10.5 dpc, decreases and acquires a first arch-like pattern in the absence of *Hoxa2* (Fig. 5). Thus, *Hoxa2* can regulate gene expression both positively and negatively, possibly by interacting with specific cofactors, in order to constitute a second arch specific pattern.

It is interesting to note that the asymmetrical distribution between the mandibular and hyoid arches of these gene transcripts is not evident in the NCC mesenchyme of 9.5 dpc embryos (data not shown), despite *Hoxa2* expression in the second arch. This is a further indication that *Hoxa2* mainly plays a later role, noticeable from 10.5 dpc onwards. Interestingly, even at 10.5 dpc, when the arch specific expression pattern has already been established, *Hoxa2* inactivation results in homeotic transformation of skeletal elements (Fig. 3). At the molecular level, induction of *Hoxa2*

deletion by TM treatment of 9.5 or even 10.5 dpc embryos equally results in a transformation of the second arch gene expression pattern to a first arch-like pattern (Fig. 5; and data not shown). This finding provides strong molecular support to the evidence of long-lasting plasticity of second arch NCCs, as discussed above. In fact, at least up until 10.5-11 dpc, NCCs are still able to undergo rapid molecular changes and switch their developmental course. In this respect, it is also noteworthy that the switch in gene expression upon *Hoxa2* inactivation can occur as rapidly as within 12 hours. Considering that tamoxifen takes approximately 6 hours from the time of administration to start accumulating in the nucleus, the time needed to induce a response on the NCC patterning can be considered to be even shorter than 12 hours. This is an indication that *Hoxa2* is likely to directly regulate some of those molecular targets. Accordingly, *Six2* has recently been proposed to be a direct target of *Hoxa2* (Kutejova et al., 2005). However, ectopic expression of *Six2* in the second arch NCCs was not sufficient to reproduce the *Hoxa2* mutant phenotype (Kutejova et al., 2005), suggesting a requirement for additional players. Indeed, our results suggest that a number of genes involved in patterning NCC derivatives may be under the direct transcriptional control of *Hoxa2* to generate a second arch-specific pattern. In this respect, the employment of our inducible system to compare second arch transcripts at different stages between wild type and mutant should allow the identification of the *Hoxa2* target genes responsible for the development of distinct structures.

References

Ahn, S. and Joyner, A. L. (2004). Dynamic changes in the response of cells to positive hedgehog signaling during mouse limb patterning. *Cell* **118**, 505-516.

Arenkiel, B. R., Tvrdik, P., Gaufo, G. O. and Capecchi, M. R. (2004). *Hoxb1* functions in both motoneurons and in tissues of the periphery to establish and maintain the proper neuronal circuitry. *Genes Dev.* **18**, 1539-1552.

Bialek, P., Kern, B., Yang, X., Schrock, M., Sosic, D., Hong, N., Wu, H., Yu, K., Ornitz, D. M., Olson, E. N. et al. (2004). A twist code determines the onset of osteoblast differentiation. *Dev. Cell* **6**, 423-435.

Bobola, N., Carapuco, M., Ohnemus, S., Kanzler, B., Leibbrandt, A., Neubuser, A., Drouin, J. and Mallo, M. (2003). Mesenchymal patterning by *Hoxa2* requires blocking Fgf-dependent activation of *Ptx1*. *Development* **130**, 3403-3414.

Couly, G., Grapin-Botton, A., Coltey, P., Ruhin, B. and Le Douarin, N. M. (1998). Determination of the identity of the derivatives of the cephalic neural crest: incompatibility between *Hox* gene expression and lower jaw development. *Development* **125**, 3445-3459.

Couly, G., Creuzet, S., Bennaceur, S., Vincent, C. and Le Douarin, N. M. (2002). Interactions between Hox-negative cephalic neural crest cells and the foregut endoderm in patterning the facial skeleton in the vertebrate head. *Development* **129**, 1061-1073.

Creuzet, S., Couly, G., Vincent, C. and Le Douarin, N. M. (2002). Negative effect of *Hox* gene expression on the development of the neural crest-derived facial skeleton. *Development* **129**, 4301-4313.

Crump, J. G., Swartz, M. E. and Kimmel, C. B. (2004). An integrin-dependent role of pouch endoderm in hyoid cartilage development. *PLoS Biol.* **2**, E244.

Danielian, P. S., Muccino, D., Rowitch, D. H., Michael, S. K. and McMahon, A. P. (1998). Modification of gene activity in mouse embryos in utero by a tamoxifen-inducible form of Cre recombinase. *Curr. Biol.* **8**, 1323-1326.

Dupe, V., Davenne, M., Brocard, J., Dolle, P., Mark, M., Dierich, A., Chambon, P. and Rijli, F. M. (1997). In vivo functional analysis of the *Hoxa-1* 3′ retinoic acid response element (3′RARE). *Development* **124**, 399-410.

Eames, B. F. and Schneider, R. A. (2005). Quail-duck chimeras reveal spatiotemporal plasticity in molecular and histogenic programs of cranial feather development. *Development* **132**, 1499-1509.

Feil, R., Wagner, J., Metzger, D. and Chambon, P. (1997). Regulation of Cre recombinase activity by mutated estrogen receptor ligand-binding domains. *Biochem. Biophys. Res. Commun.* **237**, 752-757.

Ferguson, C. A., Tucker, A. S. and Sharpe, P. T. (2000). Temporospatial cell interactions regulating mandibular and maxillary arch patterning. *Development* **127**, 403-412.

Gammill, L. S. and Bronner-Fraser, M. (2003). Neural crest specification: migrating into genomics. *Nat. Rev. Neurosci.* **4**, 795-805.

Gendron-Maguire, M., Mallo, M., Zhang, M. and Gridley, T. (1993). *Hoxa-2* mutant mice exhibit homeotic transformation of skeletal elements derived from cranial neural crest. *Cell* **75**, 1317-1331.

Grammatopoulos, G. A., Bell, E., Toole, L., Lumsden, A. and Tucker, A. S. (2000). Homeotic transformation of branchial arch identity after *Hoxa2* overexpression. *Development* **127**, 5355-5365.

Hayashi, S. and McMahon, A. P. (2002). Efficient recombination in diverse tissues by a tamoxifen-inducible form of Cre: a tool for temporally regulated gene activation/inactivation in the mouse. *Dev. Biol.* **244**, 305-318.

Helms, J. A., Cordero, D. and Tapadia, M. D. (2005). New insights into craniofacial morphogenesis. *Development* **132**, 851-861.

Hu, D., Marcucio, R. S. and Helms, J. A. (2003). A zone of frontonasal ectoderm regulates patterning and growth in the face. *Development* **130**, 1749-1758.

Hunt, P., Wilkinson, D. and Krumlauf, R. (1991). Patterning the vertebrate head: murine *Hox 2* genes mark distinct subpopulations of premigratory and migrating cranial neural crest. *Development* **112**, 43-50.

Hunter, M. P. and Prince, V. E. (2002). Zebrafish hox paralogue group 2 genes function redundantly as selector genes to pattern the second pharyngeal arch. *Dev. Biol.* **247**, 367-389.

Imai, T., Jiang, M., Chambon, P. and Metzger, D. (2001). Impaired adipogenesis and lipolysis in the mouse upon selective ablation of the retinoid X receptor alpha mediated by a tamoxifen-inducible chimeric Cre recombinase (Cre-ERT2) in adipocytes. *Proc. Natl. Acad. Sci. USA* **98**, 224-228.

Kanzler, B., Kuschert, S. J., Liu, Y. H. and Mallo, M. (1998). *Hoxa-2* restricts the chondrogenic domain and inhibits bone formation during development of the branchial area. *Development* **125**, 2587-2597.

Kimmel, R. A., Turnbull, D. H., Blanquet, V., Wurst, W., Loomis, C. A. and Joyner, A. L. (2000). Two lineage boundaries coordinate vertebrate apical ectodermal ridge formation. *Genes Dev.* **14**, 1377-1389.

Knosp, W. M., Scott, V., Bachinger, H. P. and Stadler, H. S. (2004). HOXA13 regulates the expression of bone morphogenetic proteins 2 and 7 to control distal limb morphogenesis. *Development* **131**, 4581-4592.

Krumlauf, R. (1994). Hox genes in vertebrate development. *Cell* **78**, 191-201.

Kutejova, E., Engist, B., Mallo, M., Kanzler, B. and Bobola, N. (2005). *Hoxa2* downregulates *Six2* in the neural crest-derived mesenchyme. *Development* **132**, 469-478.

Le Douarin, N. M. and Kalcheim, C. (1999). *The Neural Crest*, 2nd edn. Cambridge: Cambridge University Press.

Le Douarin, N. M., Creuzet, S., Couly, G. and Dupin, E. (2004). Neural crest cell plasticity and its limits. *Development* **131**, 4637-4650.

Lettice, L., Hecksher-Sorensen, J. and Hill, R. (2001). The role of *Bapx1* (*Nkx3.2*) in the development and evolution of the axial skeleton. *J. Anat.* **199**, 181-187.

Maconochie, M., Krishnamurthy, R., Nonchev, S., Meier, P., Manzanares, M., Mitchell, P. J. and Krumlauf, R. (1999). Regulation of Hoxa2 in cranial neural crest cells involves members of the AP-2 family. *Development* **126**, 1483-1494.

Metzger, D., Li, M. and Chambon, P. (2005). Targeted somatic mutagenesis in the mouse epidermis. *Methods Mol. Biol.* **289**, 329-340.

Noden, D. M. (1983). The role of the neural crest in patterning of avian cranial skeletal, connective, and muscle tissues. *Dev. Biol.* **96**, 144-165.

Nonchev, S., Vesque, C., Maconochie, M., Seitanidou, T., Ariza-McNaughton, L., Frain, M., Marshall, H., Sham, M. H., Krumlauf, R. and Charnay, P. (1996). Segmental expression of *Hoxa-2* in the hindbrain is directly regulated by Krox-20. *Development* **122**, 543-554.

Oliver, G., Wehr, R., Jenkins, N. A., Copeland, N. G., Cheyette, B. N., Hartenstein, V., Zipursky, S. L. and Gruss, P. (1995). Homeobox genes and connective tissue patterning. *Development* **121**, 693-705.

Otto, F., Thornell, A. P., Crompton, T., Denzel, A., Gilmour, K. C., Rosewell, I. R., Stamp, G. W., Beddington, R. S., Mundlos, S., Olsen, B. R. et al. (1997). *Cbfa1*, a candidate gene for cleidocranial dysplasia syndrome, is essential for osteoblast differentiation and bone development. *Cell* **89**, 765-771.

Pasqualetti, M. and Rijli, F. M. (2002). Developmental biology: the plastic face. *Nature* **416**, 493-494.

Pasqualetti, M., Ori, M., Nardi, I. and Rijli, F. M. (2000). Ectopic Hoxa2 induction after neural crest migration results in homeosis of jaw elements in Xenopus. *Development* **127**, 5367-5378.

Pasqualetti, M., Ren, S. Y., Poulet, M., LeMeur, M., Dierich, A. and Rijli, F. M. (2002). A *Hoxa2* knockin allele that expresses EGFP upon conditional Cre-mediated recombination. *Genesis* **32**, 109-111.

Prince, V. and Lumsden, A. (1994). *Hoxa-2* expression in normal and transposed rhombomeres: independent regulation in the neural tube and neural crest. *Development* **120**, 911-923.

Qu, S., Niswender, K. D., Ji, Q., van der Meer, R., Keeney, D., Magnuson, M. A. and Wisdom, R. (1997). Polydactyly and ectopic ZPA formation in *Alx-4* mutant mice. *Development* **124**, 3999-4008.

Ren, S. Y., Pasqualetti, M., Dierich, A., Le Meur, M. and Rijli, F. M. (2002). A *Hoxa2* mutant conditional allele generated by Flp- and Cre-mediated recombination. *Genesis* **32**, 105-108.

Rijli, F. M., Mark, M., Lakkaraju, S., Dierich, A., Dolle, P. and Chambon, P. (1993). A homeotic transformation is generated in the rostral branchial region of the head by disruption of *Hoxa-2*, which acts as a selector gene. *Cell* **75**, 1333-1349.

Robert, B., Sassoon, D., Jacq, B., Gehring, W. and Buckingham, M. (1989). *Hox-7*, a mouse homeobox gene with a novel pattern of expression during embryogenesis. *EMBO J.* **8**, 91-100.

Ruhin, B., Creuzet, S., Vincent, C., Benouaiche, L., Le Douarin, N. M. and Couly, G. (2003). Patterning of the hyoid cartilage depends upon signals arising from the ventral foregut endoderm. *Dev. Dyn.* **228**, 239-246.

Samad, O. A., Geisen, M. J., Caronia, G., Varlet, I., Zappavigna, V., Ericson, J., Goridis, C. and Rijli, F. M. (2004). Integration of anteroposterior and dorsoventral regulation of *Phox2b* transcription in cranial motoneuron progenitors by homeodomain proteins. *Development* **131**, 4071-4083.

Santagati, F. and Rijli, F. M. (2003). Cranial neural crest and the building of the vertebrate head. *Nat. Rev. Neurosci.* **4**, 806-818.

Schneider, R. A. and Helms, J. A. (2003). The cellular and molecular origins of beak morphology. *Science* **299**, 565-568.

Serbedzija, G. N., Bronner-Fraser, M. and Fraser, S. E. (1992). Vital dye analysis of cranial neural crest cell migration in the mouse embryo. *Development* **116**, 297-307.

Sgaier, S. K., Millet, S., Villanueva, M. P., Berenshteyn, F., Song, C. and Joyner, A. L. (2005). Morphogenetic and cellular movements that shape the mouse cerebellum; insights from genetic fate mapping. *Neuron* **45**, 27-40.

Shigetani, Y., Sugahara, F., Kawakami, Y., Murakami, Y., Hirano, S. and Kuratani, S. (2002). Heterotopic shift of epithelial-mesenchymal interactions in vertebrate jaw evolution. *Science* **296**, 1316-1319.

Shigetani, Y., Sugahara, F. and Kuratani, S. (2005). A new evolutionary scenario for the vertebrate jaw. *BioEssays* **27**, 331-338.

Soriano, P. (1999). Generalized lacZ expression with the ROSA26 Cre reporter strain. *Nat. Genet.* **21**, 70-71.

Stadler, H. S., Higgins, K. M. and Capecchi, M. R. (2001). Loss of Eph-receptor expression correlates with loss of cell adhesion and chondrogenic capacity in *Hoxa13* mutant limbs. *Development* **128**, 4177-4188.

Trainor, P. and Krumlauf, R. (2000). Plasticity in mouse neural crest cells reveals a new patterning role for cranial mesoderm. *Nat. Cell Biol.* **2**, 96-102.

Trainor, P. A., Ariza-McNaughton, L. and Krumlauf, R. (2002). Role of the isthmus and FGFs in resolving the paradox of neural crest plasticity and prepatterning. *Science* **295**, 1288-1291.

Trumpp, A., Depew, M. J., Rubenstein, J. L., Bishop, J. M. and Martin, G. R. (1999). Cre-mediated gene inactivation demonstrates that FGF8 is required for cell survival and patterning of the first branchial arch. *Genes Dev.* **13**, 3136-3148.

Tucker, A. S. and Lumsden, A. (2004). Neural crest cells provide species-specific patterning information in the developing branchial skeleton. *Evol. Dev.* **6**, 32-40.

Tucker, A. S., Yamada, G., Grigoriou, M., Pachnis, V. and Sharpe, P. T. (1999). Fgf-8 determines rostral-caudal polarity in the first branchial arch. *Development* **126**, 51-61.

Tucker, A. S., Watson, R. P., Lettice, L. A., Yamada, G. and Hill, R. E. (2004). *Bapx1* regulates patterning in the middle ear: altered regulatory role in the transition from the proximal jaw during vertebrate evolution. *Development* **131**, 1235-1245.

Wellik, D. M., Hawkes, P. J. and Capecchi, M. R. (2002). *Hox11* paralogous genes are essential for metanephric kidney induction. *Genes Dev.* **16**, 1423-1432.

Zervas, M., Millet, S., Ahn, S. and Joyner, A. L. (2004). Cell behaviors and genetic lineages of the mesencephalon and rhombomere 1. *Neuron* **43**, 345-357.